Biomacromol. J., Vol. 7, No. 3, 103-113, December 2021.

Biomacromolecular Journal
www.bmmj.org

Interaction of Gold Nanoparticle with Glycated Human Serum Albumin: Impact of Morphology and Different Surface Functionalization

M. Jahanshah Talab[a], M.R. Housaindokht[b,*], Z. Tavassoli[c] and B. Ranjbar[a,*]

[a]*Department of Biophysics, Faculty of Biological Sciences, Tarbiat Modares University, Tehran, Iran*

[b]*Biophysical chemistry laboratory, Department of Chemistry, Faculty of Science, Ferdowsi University of Mashhad, Mashhad, Iran*

[c]*Department of Biology, Islamic Azad University Central Tehran Branch, Tehran, Iran*

(Received 31 October 2022, Accepted 18 December 2022)

ABSTRACT

A layer of proteins covers the nanoparticles by exposure to the nanoparticles in biological fluids. The phenomenon known as biocorona can alter the nanoparticle's specific purpose. Since the usage of nanoparticles in biological issues such as drug delivery, biosensor, and photothermal has increased, evaluating nanoparticles' interactions with biomolecules is necessary. Hydrophilic polymers form a layer of water molecules that reduces the interaction potential between nanoparticles and biomolecules. In this study, the effects of gold nanoparticle morphology (spheres and rods) and surface functionalization (PEG and GSH) on glycosylated serum albumin, a model protein in diabetic patients, its secondary structure and chemical stability using circular dimorphism technique were investigated. PEG-AuNPs exhibit a larger hydrodynamic radius than GSH-AuNPs due to their large hydrophilic tails. After interaction with the protein, the nanoparticles showed less interaction with the protein due to the formation of a layer of water around them that reduces the probability of interaction with proteins. The circular dichroism also exhibits that different modified nanoparticles do not significantly influence secondary structure. The presence of nanoparticles with hydrophilic coatings, mainly polyethylene glycol with high water retention, reduce protein availability from urea in the long run and as a result will increase the ΔG_{H2O} value.

Keywords: Biocorona, Circular dichroism, Nanomaterial

INTRODUCTION

Nanotechnology development causes tremendous advances in therapeutics and diagnostics fields. Metal nanoparticles show different electronic and optical properties in comparison to bulk materials. Quantum confinement effects and high surface-to-volume ratio cause the unique properties of the nanoparticles [1,2].

Lots of investigation has been done on gold nanoparticles. The unique properties of gold nanoparticles, such as their optical properties, easy-to-make synthesis processes, and surface functionalization, enable them to be used in numerous applications like the analytical sensing, drug delivery, molecular imaging, and photothermal treatment of tumors [3-6].

*Corresponding authors. E-mail: ranjbarb@modares.ac.ir; housain@um.ac.ir

Gold nanoparticle surfaces easily interact with coherent light. As a result, conduction-band electrons oscillate. This oscillation depends on nanoparticles size, shape, degree of aggregation, and their local environment. Gold nanorod (GNR) with the intense adjustable plasmon resonance absorbs the light a thousand times more than any organic dye, which makes it favorable in biosensing [5,7,8].

By light exposure, GNR shows two-directional electron oscillations. Stronger absorption is along with the longitudinal band (> 600 nm), and the transverse band is the shorter axis one (around 520 nm). The environmental parameters can affect intensively on longitudinal band [9]. By exposure of nanoparticles to serum or plasma, protein corona is formed rapidly around the nanoparticles [10-12]. The formation of this nonspecific absorption has mainly two reasons: (i) raising in the collective entropy of the proteins on the surface of the nanoparticles (ii) nonspecific interactions between the proteins and nanoparticles [13].

The protein corona is a dynamic structure that has two-layer. The external layer (soft corona) quickly changes with the surrounding biomaterial. The inner layer (hard corona) is almost constant and irreversible due to covalent interaction [14-16].

The kinetic and protein corona composition are dependent on a wide range of factors such as characteristic properties of the environment (protein composition and concentration), physicochemical aspects of nanoparticles (surface charge of functional groups, chemical composition, morphology), and the exposure time [10,17,18]. Protein corona critically affects the nanoparticle bio identity, which is distinctive from their synthetic identity [19]. Indeed, the attached proteins cover the pristine surface of NPs, exhibit a new identification for cell distinction, and result in notably changed *in vivo* fates [20,21].

Therefore, manipulating the nanoparticles' physicochemical properties during their development, such as their size, shape, morphology, and surface chemistry, is pertinent to improve their safety, efficacy, and control over NP-protein interactions [22-24]. In diabetic cases, 52-60% of the plasma protein is Glycated Human Serum Albumin. HSA regulates the osmotic pressure, mediates lipid metabolism, and binds to free radicals. The most critical HSA function is transporting various ingredients, such as drugs and hormones. Therefore, it is a main protein in the research field and has been chosen as a model protein [25,26].

This protein has only one polypeptide chain containing 585 amino acids and most residues are in the alpha-helix structure. It has seventeen disulfide bridges, as well. Any alterations in the protein structure can hamper its functions and causes an immune response [27,28]. Glycation is the non-enzymatic process that carbohydrate moieties are added to the reactive protein residues. In this process, the Millard reaction is done between the carbonyl part of the sugar and a specific residue *via* its free amino group [29-31]. Amadori products and Schiff's bases are produced in the early stage of glycation. Advanced glycated end products (AGE), which represent a wide range of chemical structures with different biological properties, are made by additional oxidation [32-34].

Coating nanoparticles with an organic layer makes them more long-term stable biological fluids because they can overcome the attracting forces occurring between nanoparticles. Polymers having functional groups with high affinity to gold like sulfhydryl (–SH) and amino (–NH2) groups are good stabilizing agents for gold Nanoparticles [35,36]. The typical strategy for minimizing the nanoparticle surface energy is grafting hydrophilic polymers, such as PEG (polyethylene glycol) or PEEP (poly ethyl ethylene phosphate), on the nanoparticle surface [37]. Hydrophilic polymers provide a highly hydrated shell that forcefully decreases the attractive forces between nanoparticles and biomolecules.

Therefore, hydrophilic polymers such as PEG significantly increase the nanoparticle's physical stability [38]. Glutathione (GSH) is a tri-peptide (Glu-Cys-Gly) that is urgent in oxidative damage to protect intracellular components since a hydrophilic interface is formed by two free –COOH and a –NH2 group [39-41]. Herein, the interaction of gold nanoparticles with different morphology (sphere and rod) and surface functionalization (PEG and GSH) on glycated human serum albumin, a biological protein model in a diabetic individual was studied since the influence of the charge, morphology, and surface functionalization on nanoparticle efficiency has been proved.

MATERIALS AND METHODS

Chemicals

$HAuCl_4 \cdot 3H_2O$ (99.9%), NaBH4 (99%), ascorbic acid (99%), hexadecyl trimethyl ammonium bromide (CTAB) (99%), AgNO3 (99%) and glycated albumin were procured from Sigma-Aldrich (USA). Anhydrous potassium dihydrogen phosphate and dipotassium hydrogen phosphate were purchased from (Germany). All experiments were carried out in deionized water (DI).

Gold Spherical Nanoparticles and Gold Nanorods Preparation and Purification

Gold nanorods (AuNRs) were made through seed-mediated growth methods [42,43]. Add 250 µl of an aqueous 10 mM solution of $HAuCl_4$, $3H_2O$ to 7.5 ml of a saturated 95 mM cetyltrimethylammonium bromide (CTAB) solution and then adding of 600 µl of 10 mM ice-cold $NaBH_4$ aqueous solution, the seed solution was

prepared.

Then, the solution was shaken for two minutes. The tubes were kept at room temperature for about two hours. The seed step is followed by the growth step, which is briefly explained. 9.5 ml of 95 mM CTAB, 400 µl of 10 mM $HAuCl_4.3H_2O$, 60 µl of 10 mM $AgNO_3$ solutions, and 64 µl of 100 mM ascorbic acid were added, respectively. The tubes were kept undisturbed for 3 h to allow the particles growth. The nanorod solution was purified with centrifugation (14500 rpm, 5 min). After three rounds of centrifuging and washing with deionized water, the phosphate buffer (pH = 6.8) was replaced with deionized water.

Spherical gold nanoparticles (AuNSs) were prepared using the protocol described by Fenger *et al.* in which a 10 ml mixture of trisodium citrate and $HAuCl_4$ (both with 0.25 mM concentration) was prepared. 0.3 ml of ice-cold $NaBH_4$ (0.1 M) was rapidly added to the mixture of trisodium citrate and HAuCl4. The orange-red color of the solution indicated the formation of gold seeds S1. 2 h incubation time is required to seed preparation. The growth solution adds 0.25 mM of $HAuCl_4$ to 0.08 M of CTAB. Then 0.1 M of a reductant, ascorbic acid (0.25 ml), and 5 ml of seed solution S1 were added. By centrifugation at 14500 rpm for 5 min excess amount of CTAB has been separated [44].

Modification of Nanoparticles Using Thiol Compounds

In this study, PEG-SH and glutathione having thiol compounds were used to modify nanoparticles and were covalently grafted to the surface of the Au nanoparticles. In the modification approach, a ligand solution (10 × 10-4 M) was added into 1 ml of nanoparticles solution (about 150 nM), and then the resulting solution was stirred for 24 h at 4 °C. The excess PEG-SH and GSH were removed *via* centrifugation at 15 000 rpm for about 10 min. The successful modification of the nanoparticles was approved using different physicochemical techniques.

UV-Vis spectroscopy. The modified gold nanoparticles were characterized by a UV-Vis absorption spectrophotometer (Scinco UV S-2100 LabPro Plus) within the 400-900 nm wavelength range.

Transmission electron microscopy. The excess amount of modifier was removed by two rounds of centrifugation and re-dispersion in deionized water. The diluted sample was deposited and left undisturbed to evaporate the solvent on a carbon-coated copper grid. After that, Transmission Electron Microscopy (TEM) study was done with a TE 2000 Zeiss electron microscope.

Dynamic light scattering and zeta potential measurements. The ζ potentials of modified nanoparticles and hydrodynamic diameters of modified GNPs after modification and after 2 h interaction with protein solution were determined by Malvern Zetasizer Nano series ZS instrument, equipped with a HeNe laser operating at 632.8 nm.

FTIR analysis. Samples of modified nanoparticles were converted into a dry powder using a lyophilizer (LYSFME-Snijders scientific). On a NICOLET IR 100 (FT-IR), the spectra were recorded and in the 800-3800 cm^{-1} was reported to approve the modification.

Circular Dichroism Spectropolarimetry

A determined concentration of protein (2.9 µM) was mixed with different nanoparticle concentrations (0-0.66 mM). After 1 h incubation at 4 °C, far UV-CD measurements were done on JASCO Spectropolarimeter (J-715) to trace the conformational change in protein induced by different nanoparticles.

Analyzed data were reported in terms of molar ellipticity [θ] based on mean amino acids residue weight (MRW):

$$[\theta] = \theta \times 100\ MRW/Cl$$

Where C is the protein concentration in mg ml^{-1}, l is the light path length in centimeters and Θ is the measured ellipticity in degree at wavelength λ [45-47].

Equilibrium unfolding of glycated albumin with urea. The experiments of equilibrium unfolding protein were done in the presence of modified nanoparticles. In studies of protein unfolding in the presence of nanoparticles, a series of solutions containing constant amounts of free and cross-linked glycosylated albumin were incubated with different concentrations of urea (0 to 12 M) for at least 1 h. The CD region was then scanned in the far ultraviolet (UV) between 200 and 250 nm with a bandwidth of 1 nm. All experiments were performed at room temperature (25 °C).

The unfolding free energy was calculated by converting the CD UV data to the unfolding free energy (ΔGD) for each data point. The equilibrium constant "K" is calculated for a given protein concentration. Assuming a two-state unfolding mechanism, the urea-induced unfolding curve can be used to calculate the free energy of Gibb's stabilization (ΔG_{H20}) in the absence of urea by linearly extrapolating the ΔGD value to zero urea concentration [48-50].

RESULTS AND DISCUSSION

Functionalized Gold Nanoparticles Characterization

UV-Vis spectroscopy and transmission electron microscopy. Figure 1 represents transmission electron microscopy image of gold nanoparticles. According to the TEM image, the size of the monodisperse GNPs and GNRs was assessed to be 15 ± 2 nm and 30 ± 2 (length) and 10 ± 2 nm (width), respectively.

The characteristic plasmonic absorption bands of gold nanoparticles were shown in Fig. 2. Their characteristic surface plasmon resonance bands after functionalization with GSH and PEG were compared as well. A slight decrease upon functionalization was observed in the plasmonic absorption band intensity of functionalized gold nanoparticles. This decrement indicates that the sensitivity of the electron oscillation to the surrounding environment changes and confirms that the gold nanoparticle environment has changed.

Dynamic light scattering and zeta potential analysis. As electron microscopy of Au nanoparticles needs dehydrated samples, and the diameter of modified nanoparticles does not exhibit any changes, the DLS technique is applied, which is sensitive for the characterization of dispersions of nanoparticles and nanoparticle-polymer hybrids.

Because of the PEG chains' flexibility compared to GSH, PEG can reduce the Brownian motion of particles by presenting additional frictional drag and decreasing nanoparticle diffusivity compared with GSH-AuNPs [51]. The validation of loading of PEG and GSH on the AuNP surface can be proved via the zeta potential and dynamic light scattering measurements. For the positively charged CTAB-capped gold nanospheres (CTAB-AuNSs)

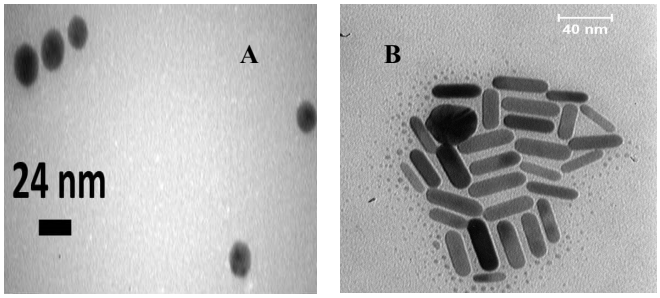

Fig. 1. TEM image of (TEM 2000 ziess) the purified (A) GNPs and (B) GNRs.

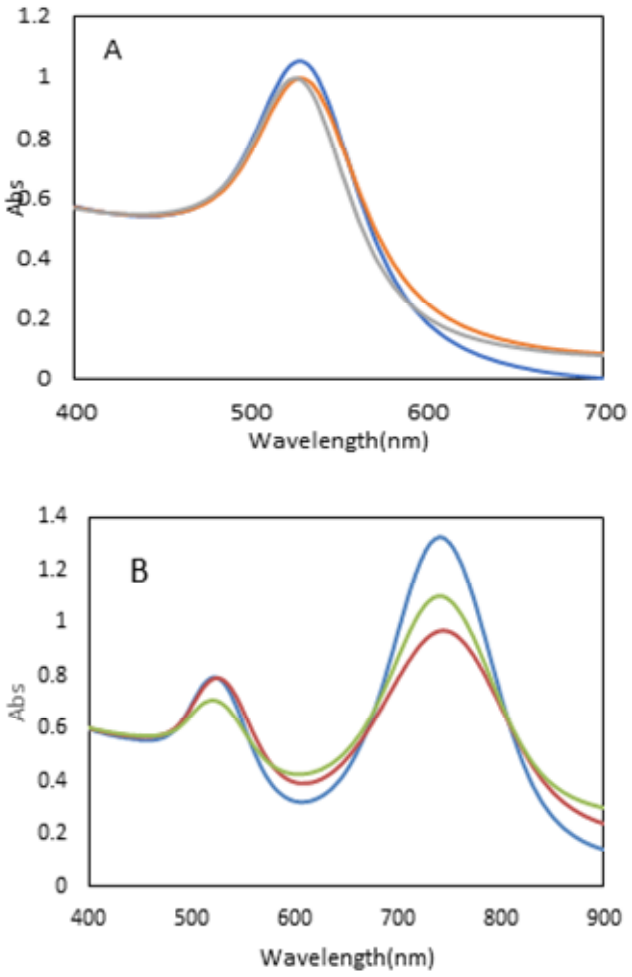

Fig. 2. Representative absorption spectra of (A) gold Nanospheres, (B) gold Nanorods dispersed in 10 mM phosphate buffer, pH 6.8; CTAB-gold Nanoparticles (blue line); PEG-gold Nanoparticles (gray line); and GSH-gold Nanoparticles (orange line).

Table 1. Different Nanoparticles' DLS and Zeta Potential before and after Functionalization with 100 mM Glutathione and PEG Concentrations

	pdI	Hydrodynamic radius (nm)	Zeta potential (mv)
CTAB-AuNSs	0.18	33.6	16.32
GSH-AuNSs	0.21	37.44	-8.05
PEG-AuNSs	0.32	284.73	-11.98
CTAB-AuNRs			20.08
GSH-AuNRs			-22.42
PEG-AuNRs			-14.30

and gold nanorods (CTAB-AuNRs), the zeta potential values were 16.33 and 20.8, respectively. As it can be seen in Table 1, after functionalizing with PEG and GSH, this parameter becomes near negative values because PEG has long hydrophilic chains with a neutral charge and GSH in pH = 6.8 has a negative charge (PEG-AuNS: -11.98, PEG-AuNR: -14.3, GSH-AuNS: -8.05, PEG-AuNR: -22.42). Before and after functionalization with PEG and GSH, measuring the mean hydrodynamic diameters of CTAB-AuNPs was done.

According to Table 1, upon functionalization, the hydrodynamics radius values of functionalized nanoparticles increased due to the presence of hydrophilic chains which attract water molecules. This increment represented that in modified nanoparticles the ζ potentials and the hydrodynamic diameters were completely different comparing to those of unmodified nanoparticles, which confirms the GNPs successful modification of nanoparticles with thiol compounds.

After successful nanoparticle modification and interaction with a protein solution, the modified nanoparticles' hydrodynamics radius did not significantly change, indicating lesser interaction with protein. This result demonstrates that coated nanoparticles with hydrophilic polymers interact with proteins lesser than CTAB-AuNPs (Table 2).

FTIR analyses. To confirm the modification of nanoparticles with PEG and GSH, the FTIR spectrum was recorded. The IR spectrum of free GSH and PEG reveals the presence of mercapto groups in 2530-2660 nm^{-1}. As shown in Fig. 3, the mercapto groups in the FTIR spectrum of GSH and PEG disappeared in that of GSH-AuNPs and PEG-AuNPS. This fact indicates that the binding of PEG and GSH to nanoparticles was done via mercapto groups, and the GNPs were successfully modified with thiol compounds.

Table 2. The Hydrodynamic Radius of Different Nanoparticles before and after Exposure to the Protein Solution. The Protein and Nanoparticle Concentrations are 2.9 μM and 150 μM Respectively

System	Hydrodybamic radius (d nm)
CTAB-AuNSs	76
(CTAB-AuNSs)pr	55.98
PEG-AuNSs	288.73
(PEG-AuNSs)pr	288.28
GSH-AuNSs	61.12
(GSH-AuNSs)pr	60.61

Secondary Structure of Glycated Human Albumin

Circular Dichroism (CD) is a beneficial method to detect some conformational alterations in the structure of macromolecules [52,53]. For glycated HSA at pH 7.0 two negative minima in the ultraviolet region at 208 and 222 nm were observed in the CD spectrum, which represents an α-helical structure of the protein [54]. Analysis of the far-UV CD spectrum of glycated albumin confirms mixed α/β type secondary structures.

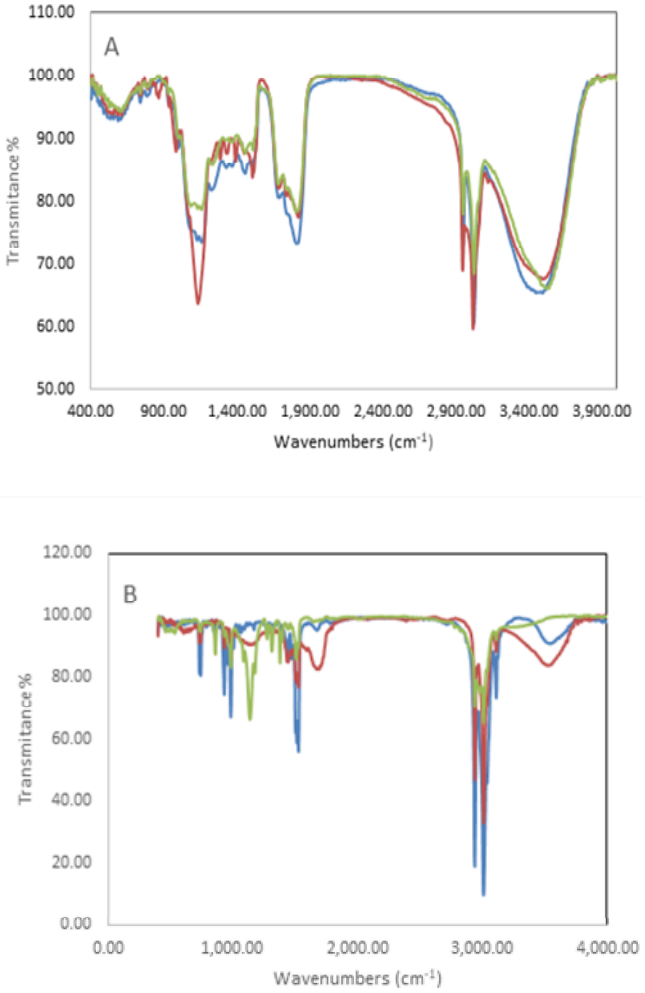

Fig. 3. Representative FTIR spectra of (A) gold Nanospheres, (B) gold Nanorods; ctab-gold Nanoparticles (blue line); PEG-gold Nanoparticles (gray line); and GSH-gold Nanoparticles (orange line).

In Fig. 4 far-UV CD spectra of glycated human albumin without and in the presence of different gold nanoparticles are shown, demonstrating the specificity of the interaction of a chiral molecule with polarized light. The characteristic peaks of 208 and 222 nm, can be explained by the $\pi \rightarrow \pi^*$ and $n \rightarrow \pi^*$ (respectively) transition of the peptide bond, which is representative of protein compactness. After adding nanoparticles, the peaks showed gentle changes, indicating a mild significant change in protein secondary structure and helical content.

Equilibrium unfolding of glycated albumin with urea. Changes in the secondary structure were used to determine the equilibrium constant (K_{eq}) for the folding-unfolding reaction to study protein unfolding by urea. Far-UV CD analysis was carried out to assess the effect of modified nanoparticles on changing the protein structure induced by urea.

Based on the denaturant concentration, urea in this study can render a protein to be either fold or unfold. The folded/unfolded fraction of protein is determined [55,56]. Figure 5 shows the impact of increasing urea concentration on the molecular ellipticity at 222 nm by assuming a two-state model (nature and denature states). The molecular ellipticity was reduced from 2.0 M to 8 M and a complete around 12 M urea, illustrating an unfolded protein.

For the folding-unfolding reaction, the equilibrium constant (K_{eq}) was calculated by analyzing the sigmoidal curves. Protein stabilities in the presence of each nanoparticle could be obtained by calculating the equilibrium constant in different denaturant concentrations, representing changes in the unfolding energies.

Figure 6 shows the Gibbs free energy changes plotted versus different denaturant concentrations. The m-value is calculated *via* the slope of the linear plots which reflects the difference in the accessible surface area between the unfolded and folded state of the protein. The bigger this value, the higher the degree of structural stability [42].

As can be seen in Table 3, the m-value of protein in the presence of modified nanoparticles increases. Comparing the m-value between PEG-(gold Nanoparticles) and GSH-(gold Nanoparticles) revealed that PEG can increase this parameter more than GSH in both nanorods and nanospheres.

Gibbs free energy (ΔG) was calculated to investigate the conformational stability of glycated albumin. The free energy change is, therefore, a reliable indicator of the spontaneity of a process. In the absence of denaturant (ΔGH_2O), the far-UV CD was utilized to calculate the Gibbs free energy which is the indicator of the conformational stability of the protein (Table 3).

As seen in Table 3, for the modified gold nanosphere in the absence of denaturant, the Gibbs free energy increases, which is an indicator of the stability of the protein in the presence of a modified gold nanosphere with PEG and

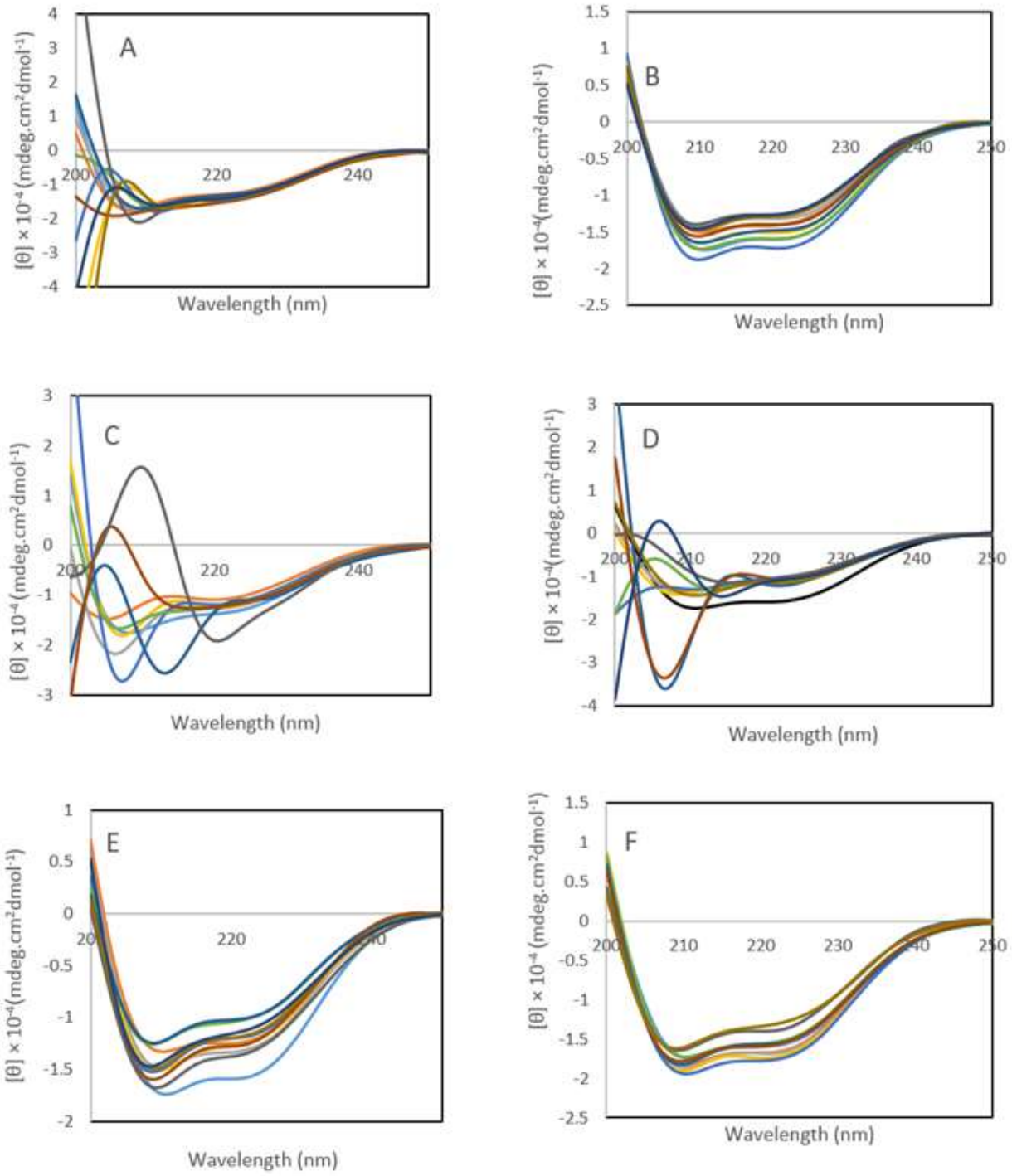

Fig. 4. Far-UV CD spectra of glycated albumin in 0.01 M potasium phosphate buffer, pH 6.8. in different (A) ctab-gold nanosphere; (B) PEG-gold nanosphere; (C) GSH-gold nanosphere; (D) CTAB-gold nanorod; (E) PEG-gold nanorod; (F) GSH-gold nanorod concentrations (0-0.66 mM). The protein concentration is 2.9 µM.

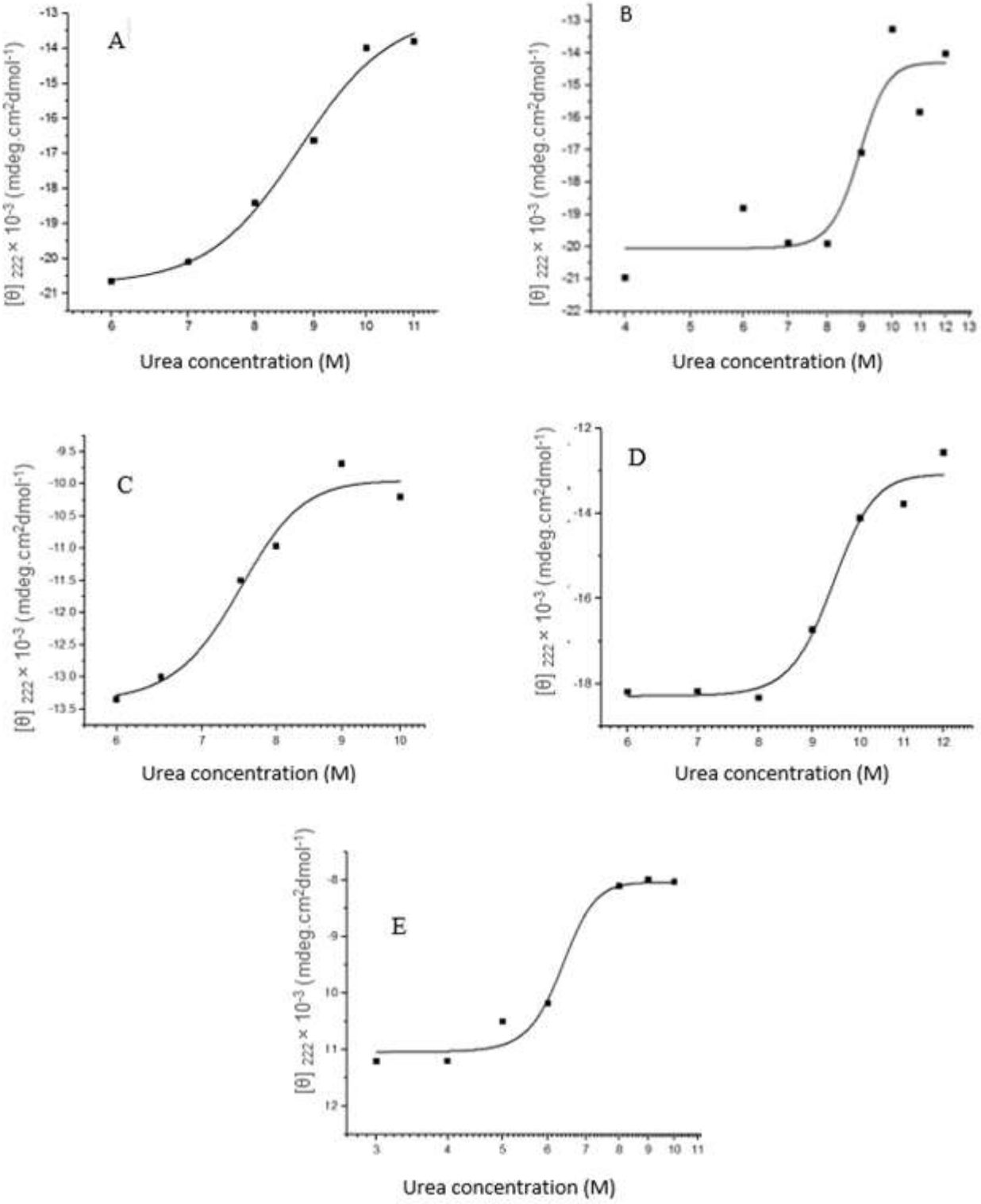

Fig. 5. the effect of urea concentration on molecular ellipticity at 222 nm of (A) glycated albumin; (B) glycated albumin-GSH-AuNSs; (C) glycated albumin-PEG-AuNSs; (D) glycated albumin-PEG-AuNRs; (E) glycated albumin-GSH-AuNRs. The protein and nanoparticle concentrations are 2.9 μM and 150 μM respectively.

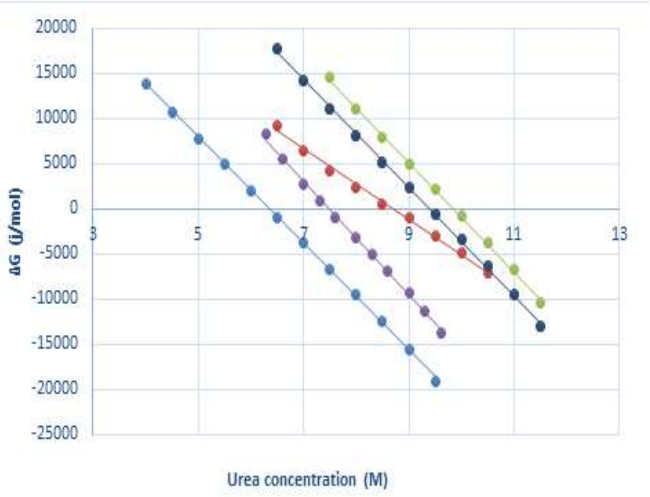

Fig. 6. Thermodynamic analysis of unfolding data. Unfolding free energy change in (red line) glycated albumin; (gray line) glycated albumin-GSH-AuNSs; (yellow line) glycated albumin-PEG-AuNSs; (dark blue) glycated albumin-PEG-AuNRs; (blue line) glycated albumin-GSH-AuNRs is plotted versus different denaturant concentration**.** The protein and nanoparticle concentrations are 2.9 µM and 150 µM respectively. The urea concentration increases from 0 to 12 M.

Table 3. Thermodynamic Parameters of AuNRs-glycated Albumin and AuNSs-glycated Albumin. The Protein and Nanoparticle Concentrations are 2.9 µM and 150 µM Respectively

	ΔG H2O ($J\ mol^{-1}$)	m-value ($J\ mol^{-1}\ M^{-1}$)
pr-urea	33093 ± 2%	-3886 ± 2%
Pr-(PEG-AuNRs) Urea	57937 ± 2%	-6023 ± 2%
Pr-(GSH-AuNRs) Urea	38296 ± 2%	-5994 ± 2%
Pr-(PEG-AuNSs) Urea	47518 ± 3%	-6344 ± 3%
Pr-(GSH-AuNSs) Urea	60299 ± 3%	-5869 ± 3%

GSH. In the case of the gold nanorod, both modified nanorods increase the protein chemical stability, but the PEG-AuNRs increase the protein stability to a greater extent than GSH-AuNRs.

CONCLUSION

Gold nanostructures with PEG and GSH functionalization show distinct changes in the stability and structure of glycated HSA. CD data showed that nanoparticles modified with hydrophilic polymers induced slight conformational changes in the protein secondary structure and the protein retained most of its helical structure. Variation in protein stability based on the free energy of unfolding was in the order HSA-GSH-AuNSs > HSA-PEG-AuNRs > HSA-PEG-AuNSs > HSA-GSH-AuNRs. PEG-AuNPs exhibited higher hydrodynamic values comparing to CTAB-capped and GSH-capped counterparts. Although the presence of nanoparticles affects the secondary structure of the protein to some extent, incubating the protein with 0.15 mM nanoparticles prior to adding different concentrations of urea increases the ΔGH2O parameter. The presence of nanoparticles with hydrophilic coatings, especially polyethylene glycol with higher water retention, prevents urea from reaching the protein ultimately and thus increases the ΔG_{H2O} value. This research gives us in-depth insights into the interaction of different nanoparticles and the most abundant protein in diabetic blood, glycated albumin. This investigation showed that changing the morphology and surface-coated nanoparticles can create a system with the slightest interaction with biological macromolecules. The DLS data after interaction with proteins confirm that modified nanoparticles interact lesser than CTAB-AuNPS.

REFERENCES

[1] S. Abe, K. Kajikawa, Phys. Rev. B 74 (2006) 035416.
[2] H. Bönnemann, K. Nagabhushana, Journal of New Materials for Electrochemical Systems 7 (2004) 93.
[3] Z. Ma, H. Xia, Y. Liu, B. Liu, W. Chen, Y. Zhao, Chinese Science Bulletin 58 (2013) 2530.
[4] H. He, C. Xie, J. Ren, Analytical chemistry 80 (2008) 5951.
[5] X. Huang, P.K. Jain, I.H. El-Sayed, M.A. El-Sayed, Gold Nanoparticles: Interesting Optical Properties and Recent Applications in Cancer Diagnostics and Therapy, 2007.
[6] L. Vigderman, B.P. Khanal, E.R. Zubarev, Advanced

Materials 24 (2012) 4811.
[7] A.A. Oraevsky, Gold and Silver Nanoparticles as Contrast Agents for Optoacoustic Tomography, Photoacoustic Imaging and Spectroscopy, CRC Press, 2017.
[8] K. Urbanska, B. Romanowska-Dixon, Z. Matuszak, J. Oszajca, P. Nowak-Sliwinska, G. Stochel, Acta Biochimica Polonica 49 (2002) 387.
[9] P.K. Jain, X. Huang, I.H. El-Sayed, M.A. El-Sayed, Accounts of Chemical Research 41 (2008) 1578.
[10] C.D. Walkey, J.B. Olsen, H. Guo, A. Emili, W.C. Chan, Journal of the American Chemical Society 134 (2012) 2139.
[11] M. Lundqvist, J. Stigler, G. Elia, I. Lynch, T. Cedervall, K.A. Dawson, Proceedings of the National Academy of Sciences 105 (2008) 14265.
[12] M.P. Monopoli, D. Walczyk, A. Campbell, G. Elia, I. Lynch, F. Baldelli Bombelli, K.A. Dawson, Journal of the American Chemical Society 133 (2011) 2525.
[13] R. Podila, R. Chen, P.C. Ke, J. Brown, A. Rao, Applied Physics Letters 101 (2012) 263701.
[14] I. Lynch, A. Salvati, K.A. Dawson, Nature Nanotechnology 4 (2009) 546.
[15] S. Milani, F. Baldelli Bombelli, A.S. Pitek, K.A. Dawson, J. Radler, ACS Nano 6 (2012) 2532.
[16] J. Wang, U.B. Jensen, G.V. Jensen, S. Shipovskov, V.S. Balakrishnan, D. Otzen, J.S. Pedersen, F. Besenbacher, D.S. Sutherland, Nano Letters 11 (2011) 4985.
[17] E. Casals, T. Pfaller, A. Duschl, G.J. Oostingh, V.F. Puntes, Small 7 (2011) 3479-3486.
[18] S. Tenzer, D. Docter, S. Rosfa, A. Wlodarski, J.r. Kuharev, A. Rekik, S.K. Knauer, C. Bantz, T. Nawroth, C. Bier, ACS Nano 5 (2011) 7155.
[19] F. Charbgoo, M. Nejabat, K. Abnous, F. Soltani, S.M. Taghdisi, M. Alibolandi, W.T. Shier, T.W. Steele, M. Ramezani, Journal of Controlled Release 272 (2018) 39.
[20] Q. Peng, H. Mu, Journal of Controlled Release 225 (2016) 121.
[21] A. Salvati, A.S. Pitek, M.P. Monopoli, K. Prapainop, F.B. Bombelli, D.R. Hristov, P.M. Kelly, C. Åberg, E. Mahon, K.A. Dawson, Nature Nanotechnology 8 (2013) 137.
[22] Y.-M. Cho, Y. Mizuta, J.-I. Akagi, T. Toyoda, M. Sone, K. Ogawa, Journal of Toxicologic Pathology 31 (2018) 73.
[23] D.D. Jurašin, M. Ćurlin, I. Capjak, T. Crnković, M. Lovrić, M. Babič, D. Horák, I.V. Vrček, S. Gajović, Beilstein Journal of Nanotechnology 7 (2016) 246.
[24] X. Hong, J. Wen, X. Xiong, Y. Hu, Environmental Science and Pollution Research 23 (2016) 4489.
[25] T. Peters Jr, All about Albumin: Biochemistry, Genetics, and Medical Applications, Academic Press, 1995.
[26] J. Anguizola, R. Matsuda, O.S. Barnaby, K. Hoy, C. Wa, E. DeBolt, M. Koke, D.S. Hage, Clinica Chimica Acta 425 (2013) 64.
[27] L. Mihajlovic, J. Radosavljevic, E. Nordlund, M. Krstic, T. Bohn, J. Smit, J. Buchert, T.C. Velickovic, Food & Function 7 (2016) 2357.
[28] A.S. Rosenberg, The AAPS journal 8 (2006) 501.
[29] P. Rondeau, G. Navarra, F. Cacciabaudo, M. Leone, E. Bourdon, V. Militello, Biochimica et Biophysica Acta (BBA)-Proteins and Proteomics 1804 (2010) 789.
[30] S. Zarina, H.-R. Zhao, E. Abraham, Molecular and Cellular Biochemistry 210 (2000) 29.
[31] S.V. Chetyrkin, M.E. Mathis, A.-J.L. Ham, D.L. Hachey, B.G. Hudson, P.A. Voziyan, Free Radical Biology and Medicine 44 (2008) 1276.
[32] V.M. Monnier, D.R. Sell, R.H. Nagaraj, S. Miyata, S. Grandhee, P. Odetti, S.A. Ibrahim, Diabetes 41(Supplement_2) (1992) 36.
[33] H. Vlassara, Annals of the New York Academy of Sciences 1043 (2005) 452.
[34] P. Ulrich, A. Cerami, Recent Progress in Hormone Research 56 (2001) 1.
[35] S.-D. Li, L. Huang, Journal of Controlled Release: Official Journal of the Controlled Release Society 145 (2010) 178.
[36] M.H. Jazayeri, H. Amani, A.A. Pourfatollah, H. Pazoki-Toroudi, B. Sedighimoghaddam, Sensing and Bio-sensing Research 9 (2016) 17.
[37] P.C. Ke, S. Lin, W.J. Parak, T.P. Davis, F. Caruso, ACS Nano 11 (2017) 11773.
[38] C. Branca, S. Magazu, G. Maisano, F. Migliardo, P. Migliardo, G. Romeo, The Journal of Physical Chemistry B 106 (2002) 10272.
[39] R.P. Briñas, M. Hu, L. Qian, E.S. Lymar, J.F. Hainfeld,

Journal of the American Chemical Society 130 (2008) 975.

[40] S. Basu, T. Pal, Journal of Nanoscience and Nanotechnology 7 (2007) 1904.

[41] F. Chai, C. Wang, T. Wang, L. Li, Z. Su, ACS Appl. Mater. Interfaces 2 (2010) 1466.

[42] T.T. Moghadam, B. Ranjbar, K. Khajeh, S.M. Etezad, K. Khalifeh, M.R. Ganjalikhany, International Journal of Biological Macromolecules 49 (2011) 629.

[43] M.S. Naderi, T.T. Moghadam, K. Khajeh, B. Ranjbar, International Journal of Biological Macromolecules 107 (2018) 297.

[44] R. Fenger, E. Fertitta, H. Kirmse, A.F. Thünemann, K. Rademann, Physical Chemistry Chemical Physics 14 (2012) 9343.

[45] B. Ranjbar, P. Gill, Chemical Biology & Drug Design 74 (2009) 101.

[46] M.R. Ganjalikhany, B. Ranjbar, S. Hosseinkhani, K. Khalifeh, L. Hassani, Journal of Molecular Catalysis B: Enzymatic 62 (2010) 127.

[47] N. Shahbazi, S. Hosseinkhani, B. Ranjbar, Sensors and Actuators B: Chemical 253 (2017) 794.

[48] C. Pace, Methods in enzymology, Elsevier, 1986.

[49] H. Shukla, R. Shukla, A. Sonkar, T. Pandey, T. Tripathi, Scientific Reports 7 (2017) 1.

[50] B. Dabirmanesh, K. Khajeh, B. Ranjbar, F. Ghazi, A. Heydari, Journal of Molecular Liquids 170 (2012) 66.

[51] H. Liu, T.L. Doane, Y. Cheng, F. Lu, S. Srinivasan, J.J. Zhu, C. Burda, Particle & Particle Systems Characterization 32 (2015) 197.

[52] I. Protasevich, B. Ranjbar, V. Lobachov, A. Makarov, R. Gilli, C. Briand, D. Lafitte, J. Haiech, Biochemistry 36 (1997) 2017.

[53] K. Khajeh, B. Ranjbar, H. Naderi-Manesh, A.E. Habibi, M. Nemat-Gorgani, Biochimica et Biophysica Acta (BBA)-Protein Structure and Molecular Enzymology 1548 (2001) 229.

[54] T. Sen, K.K. Haldar, A. Patra, The Journal of Physical Chemistry C 112 (2008) 17945.

[55] D. Mendez, R. Jensen, L. McElroy, J.M. Pe na, R.M. Esquerra, Arch. Biochem. Biophys. 444 (2005) 92.

[56] F. Karbassi, K. Haghbeen, A. Saboury, B. Ranjbar, A. Moosavi-Movahedi, Colloids. Surf. B. 32 (2003) 137.